Title

Alterations in cortical and thalamic connections of somatosensory cortex following early loss of vision

Permalink

https://escholarship.org/uc/item/80w2m8nw

Journal

The Journal of Comparative Neurology, 527(10)

ISSN

1550-7149

Authors

Dooley, James C
Krubitzer, Leah A

Publication Date

2019-07-01

DOI

10.1002/cne.24582

Peer reviewed

Alterations in cortical and thalamic connections of somatosensory cortex following early loss of vision

James C Dooley[1] and **Leah A. Krubitzer**[2,3]

[1]Department of Psychological and Brain Sciences, University of Iowa, Iowa City, IA

[2]Center for Neuroscience, University of Iowa, Iowa City, IA

[3]Department of Psychology, University of California, Davis, CA

Abstract

Early loss of vision produces dramatic changes in the functional organization and connectivity of the neocortex in cortical areas that normally process visual inputs, such as the primary and second visual area. This loss also results in alterations in the size, functional organization and neural response properties of the primary somatosensory area, S1. However, the anatomical substrate for these functional changes in S1 have never been described. In the present investigation, we quantified the cortical and subcortical connections of S1 in animals that were bilaterally enucleated very early in development, prior to the formation of retino-geniculate and thalamocortical pathways. We found that S1 receives dense inputs from novel cortical fields, and that the density of existing cortical and thalamocortical connections was altered. Our results demonstrate that sensory systems develop in tandem and that alterations in sensory input in one system can affect the connections and organization of other sensory systems. Thus, therapeutic intervention following early loss of vision should focus not only on restoring vision, but also on augmenting the natural plasticity of the spared systems.

Graphical Abstract

Correspondence to: Leah A Krubitzer, University of California, Davis, Center for Neuroscience, 1544 Newton Court, Davis, CA 95618, Phone: 530 757 8560, Fax: 530 757 8827, lakrubitzer@ucdavis.edu.
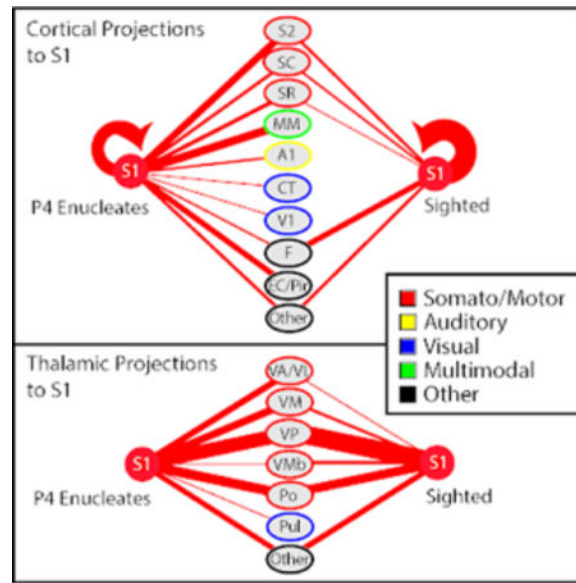
Introduction:

When the ratio of incoming sensory inputs to the developing neocortex is altered, as with congenital blindness, both the organization and connectivity of the neocortex that would normally process visual inputs are drastically changed. This has been well-demonstrated in experimental studies that remove input from the retina during early development, well before visual pathways have formed. For example, in short-tailed opossums that were bilaterally enucleated at postnatal day 4 (P4), before retinal projections have reached the optic chiasm, all of what would normally be visual cortex (V1 and V2; see Table of abbreviations) contains neurons responsive to auditory and somatosensory stimulation (Kahn & Krubitzer, 2002), and V1 receives inputs from cortical and thalamic structures normally associated with auditory and somatosensory processing (Karlen et al., 2006). Similar findings have also been described for anophthalmic mice in which *c-Fos* was used to demonstrate that both the dorsal division of the lateral geniculate nucleus (LGd) and visual cortex are activated by auditory stimulation (Chabot et al., 2007). Further, thalamic connections of V1 are altered in anophthalmic mice, but not to the same extent as in bilaterally enucleated *Monodelphis* (Charbonneau et al., 2012). With early loss of auditory input, as in congenitally deaf cats, similar types of functional and anatomical changes are observed. These cats perform better on visual discrimination tasks, and this appears to be mediated by the posterior auditory field (PAF; Lomber et al., 2010). These functional differences are accompanied by alterations in both cortical and subcortical connections of PAF (Butler et al., 2017).

The annexation of visual cortex by the spared sensory systems has also been demonstrated in congenitally blind humans using non-invasive imaging techniques. For example, visual cortex is activated under a variety of non-visual tasks including braille reading (Gizewski et al., 2003), sound localization (Arnott et al., 2013; Gougoux et al., 2005), and language processing (Bedny et al., 2015; Ricciardi et al., 2014 for review). Coincident with these functional changes, the behavioral manifestation of early loss of vision is also thoroughly documented in humans. Blind individuals perform better than sighted controls on tactile discrimination tasks (Norman & Bartholomew, 2011), somatosensory perceptual processing (Bhattacharjee et al., 2010), thermal discrimination (Slimani et al., 2015), and sound localization (Lewald, 2013; Vercillo et al., 2015). Interestingly, some individuals with congenital blindness become experts in echolocation, and this ability appears to be mediated by what would normally be visual cortex (Kolarik, et al., 2017, see Thaler & Goodale, 2016).

Most studies that examine early loss of vision focus almost exclusively on the impact of this loss on visual areas of the neocortex. Yet normal sensory development and processing rely on the integration of inputs across sensory systems (Sieben et al., 2015). Thus, one might expect that the loss of one sensory system will cause changes in connectivity, functional organization and neural response properties across a wide expanse of the neocortex, and that the extent of this reorganization will be dependent on the developmental time point at which the loss occurred. In fact, cross modal plasticity has been demonstrated in rats in which the whiskers were trimmed early in postnatal development. In these animals, connections between the primary visual (V1) and somatosensory (S1) areas were altered and functional multisensory enhancement between these fields was absent (Sieben et al., 2015). Alterations in both thalamocortical and cortico-cortical connections of primary sensory fields have also been observed with postnatal sensory loss in gerbils (Henschke et al., 2018), and in the cortical connections of mice that were bilaterally enucleated at birth (Abbott et al., 2015). Thus, even after the onset of spontaneous activity and the establishment of thalamocortical connections, loss of sensory driven input can have a rather large effect on the cortical connections of both the targeted and non-targeted primary sensory fields as well as their thalamocortical connections.

As noted above, there are a few studies in anophthalmic mice and bilaterally enucleated opossums in which sensory loss occurred before the onset of spontaneous activity and before thalamocortical connections are established, but to date, none have examined the effects of such a loss on the connections and functional organization of non-targeted primary sensory areas. In early bilaterally enucleated opossums we demonstrated that unlike sighted animals, the primary somatosensory area had a large percentage of recording sites in which neurons responded to both somatosensory and auditory stimulation (Kahn & Krubitzer, 2002; Karlen et al., 2006; Figure 1b). Further, recent work in our laboratory characterizes these functional changes in S1; the receptive fields of neurons were smaller and the ability of individual neurons to detect single whisker stimulation was increased (Ramamurthy & Krubitzer, 2018). Although it is likely that these functional alterations in S1 are the result of altered connectivity at multiple levels of the nervous system, there are no studies that examine the connections of the primary somatosensory cortex following early loss of vision.

Given the previous functional, anatomical and behavioral changes that occur with congenital blindness in animal models and humans, we hypothesize that early loss of vision will generate alterations in both cortical and subcortical connections of the preserved sensory systems. The goal of the current investigation is to examine and quantify the cortico-cortical and thalamocortical connections of the primary somatosensory area in short-tailed opossums (*Monodelphis domestica*) enucleated during early neurodevelopment (P4). At this stage, the retina is composed of an immature ganglion cell layer and cytoblast layer (Djavadian et al., 2006; Sakaguchi et al., 2008); retinal ganglion cell axons have yet to reach the optic chiasm (Taylor & Guillery, 1994) and thalamocortical projections have not yet reached the cortex (Molnár et al, 1998; Figure 2). From a larger perspective, these studies allow us to appreciate how different sensory contexts in which the individual develops manifest as anatomical and functional alterations to the neocortex, and how this, in turn, impacts the sensory-mediated behavior that the neocortex generates.

Methods:

Eight short-tailed opossums (weighing 73–165 grams) were enucleated on postnatal day 4 (P4) and allowed to develop to adulthood (> 180 days of age). Of these, 5 (2 males and 3 females) were used to determine the connections of S1, and 3 were used exclusively for histology. Connections were related to histologically processed tissue and the density of connections in different cortical fields and thalamic nuclei were quantified. Data on cortical connections and subcortical connections of S1 in seven sighted controls is from previously published studies (Dooley et al., 2013; Dooley et al., 2014). Details of the location, volume, and tracers injected in enucleated animals are in Table 1. All animals (including pregnant mothers) were housed in standard laboratory conditions, with food and water available ad libitum, and maintained on a 14/10 h light/dark cycle. All protocols were approved by the Institutional Animal Care and Use Committee of the University of California, Davis, and all experiments were performed under the National Institutes of Health's guidelines for the care of animals in research.

Enucleation surgery

Expectant mothers were checked for pups daily during the lights-on period. All animals were enucleated four days after birth (P4). Enucleation methods have been described previously (Kahn & Krubitzer, 2002; Karlen et al., 2006; Karlen & Krubitzer, 2009). Briefly, mothers were anesthetized with Alfaxan (25 mg/kg, IM), and individual pups were anesthetized by hyperthermia. Once anesthetized, the thin layer of skin covering one eye was gently cut using fine dura scissors, the eye was removed, and the skin was secured with surgical glue. Following completion of all enucleations, the mother was returned to her home cage. Animals remained with their mother until weaning (7–8 weeks of age), weaned siblings were housed together until 100 – 120 days of age, and then housed individually until tracing studies were performed. Following the completion of the studies, eye sockets were investigated to ensure the eye was completely removed.

Injections of anatomical tracers

Using sterile procedures, five injections of retrograde neuroanatomical tracers were placed in S1 of enucleated animals (Table 1). Procedures for making injections of anatomical tracers into S1 have been described previously for sighted opossums (Dooley et al., 2013, 2014). Briefly, anesthesia was induced in adult animals using 5% isoflurane, animals were placed in a stereotaxic apparatus, and isoflurane (1–3%) was delivered via a fitted mask to maintain a surgical plane of anesthesia. Dexamethasone (1.0 mg/kg, IM) and atropine (0.04 mg/kg, IM) were administered to reduce inflammation. A 2% lidocaine solution was injected at the midline of the scalp, the animal's head was shaved, and respiration and body temperature were monitored throughout the procedure.

A rostrocaudal incision was made at the midline of the scalp, the skin and temporal muscle were retracted. A small hole was drilled over S1, the dura over the injection site was opened with a fine needle, and a Hamilton syringe custom-fitted with a pulled glass pipette beveled to a fine tip was lowered ~300 to 400 μm into cortex. Either 0.3 μL of 10% Fluoro-emerald (FE, Invitrogen, Carlsbad, CA), Fluoro-ruby (FR, Invitrogen, Carlsbad, CA), or 0.15 μL of cholera toxin Subunit-B (CTB; Sigma-Aldrich, St. Louis, MO) was pressure-injected in several small increments into the cortex over a 10 to 15-minute time period. Following the injection, the craniotomy was covered with bone wax, and the temporal muscle and skin were sutured. Antibiotics (Baytril, 5 mg/kg, IM) and analgesics (buprenorphine; 0.03 mg/kg, IM) were administered before recovery from anesthesia. Analgesics continued to be administered twice daily for 2 days, and animals recovered for 7 days to allow for transport of the tracer. Animals were then euthanized with an overdose of sodium pentobarbital (Beuthanasia; >250 mg/kg, IP), transcardially perfused with 0.9% saline followed by 2–4% paraformaldehyde in phosphate buffer (pH 7.4), and finally 2–4% paraformaldehyde in 10% phosphate-buffered sucrose.

Antibody characterization

We used parvalbumin immunohistochemistry (Sigma-Aldrich, RRID: AB_477329) to aid in the identification of areal boundaries in cortex and nuclear boundaries in thalamus, as well as vGluT2 immunohistochemistry (Millipore, RRID: AB_2187552) to further aid nuclear boundaries in thalamus. Both of these antibodies have been previously used in *Monodelphis domestica* (Olkowicz et al., 2008; Wong and Kaas, 2009; Dooley et al., 2015; Ramamurthy and Krubitzer, 2016). Details of the immunohistochemical protocol used have been described previously (Seelke et al., 2012). The staining pattern observed for both of these antibodies in sighted animals is comparable with previous studies in both short-tailed opossums and other small mammals. Further, western blots on short-tailed opossum brain extracts have detected a band of the expected size (Olkowicz et al., 2008; Ramamurthy and Krubitzer, 2016). Controls where the primary antibody was not used did not show any nonspecific staining. Table 2 provides details about the antibodies and dilutions used in the present study.

Histology

Following perfusion, brains were extracted, and cortex was separated from all subcortical structures. The hippocampus and basal ganglia were dissected from the cortical

hemispheres, and cortices were manually flattened between glass slides. Brains were post-fixed in 4% paraformaldehyde for 30–120 minutes and then remained in 30% phosphate-buffered sucrose for 12–48 hours. The flattened cortex was then sectioned at 30 μm using a freezing microtome. Alternating sections were stained for myelin (Gallyas, 1979) and PV, and when applicable, CTB or mounted for fluorescent microscopy. Every section in the series stained for CTB or mounted for fluorescent microscopy was analyzed (see below). As a result, 33% of cortical sections were analyzed for labeled cell bodies.

Subcortical structures were post-fixed, submerged in sucrose for 12–48 hours, and sectioned coronally at 30 μm. Tissue was divided into 4 series: (1) cytochrome oxidase (CO; Wong-Riley, 1989), (2) fluorescent microscopy, (3) CTB, and (4) either PV or Nissl. As with cortical sections, all series mounted for fluorescent microscopy or stained for CTB were reconstructed. Thus, 33% of thalamic sections were analyzed for labeled cell bodies. In brains for which only histological processing was performed, brains were divided into 3 series, and were stained for CO, PV, and vGluT2.

Data Analysis

Injections sites and cortical field boundaries were reconstructed as described previously (Dooley et al., 2013, 2014). Only cases in which the core and halo of the injections site were restricted to S1 were used in our analysis. For the cortex, the location of anatomical boundaries was determined from the entire series of myelin and/or PV stained sections, and the series was combined into a single reconstruction (Figure 3a, b; for details see Seelke et al., 2012). In all cases, cortical injections spanned all cortical layers and did not extend into the underlying white matter. For all tracers, neurons were considered labeled if the soma could be clearly identified (Figure 3c-e). Labeled cells were plotted using an X/Y stage encoding system (MD Plot, Minnesota Datametrics, St. Paul, MN) mounted to a fluorescent microscope. Tissue outlines, blood vessels, and artifacts were plotted, which allowed these sections to be aligned to the anatomical boundaries determined from the Nissl, CO, PV or vGluT2 stained tissue, creating a comprehensive reconstruction of the neocortex containing the injection site, injection halo, labeled cells and architectonic boundaries. Labeled cells were identified in 6–8 sections of cortical tissue in all cases where labeled cell bodies could be reliably identified (Table 1). To ensure that we captured both the center of the injection and the injection halo, and to standardize the excluded region of cortex across different injections, no neurons within 250 μm of the center of the injection site were included in our neuron counts (see below) of cells projecting to the core of the injection site (Figure 3b, c).

For thalamic tissue, photographs of stained tissue were used to reconstruct anatomical boundaries of the entire series of thalamic sections. Using similar landmarks to those used in cortical tissue, labeled cells were directly related to the anatomical boundaries of adjacent sections. In all cases, labeled cells were identified through the entire series which contained labeled neurons; about 8–10 thalamic sections (Table 1).

Corticocortical connections were quantified by counting all of the labeled cells in the injected cortical hemisphere, and calculating the percentage of cells of that total number that were identified in each cortical area. Likewise, all of the labeled cells in the thalamus were counted, and the percentage of labeled cells of that total number that were found in each

thalamic nucleus was calculated. Expressing these values as a percent allowed us to normalize the data for different tracers and for injections of different sizes. In addition, this quantification allowed us to determine connection strength for each area or nucleus as follows: Strong: > 10%; Moderate: 9% to 3%; Weak: 3% to 1% but present in all cases; Intermittent: < 3% and not present in all cases. This metric of connection strength has been used previously (Dooley et al., 2013, 2014).

Statistical Tests

Differences between percentages of labeled cells in different cortical areas and different thalamic nuclei, between enucleates and sighted controls, were compared using a 2-sample Student's t-test. Alpha was set to P = 0.05.

Results:

In the following results we first describe and quantify the cortical and thalamocortical connections of S1 and directly compare these with previous results in sighted opossums. We then describe the architectonically defined boundaries of cortical fields and thalamic nuclei using a variety of different stains.

Corticocortical connections of S1 in enucleates

Injections of retrograde anatomical tracers were placed into S1 and labeled neurons resulting from these injections were assigned to different cortical fields using histologically processed tissue (see below). The percentage of labeled cells, as well as the absolute number of cells in each cortical field for each case can be found in Table 3. These connections were then quantified and compared to the cortical connections of S1 in sighted controls (Figures 4 and 5). While many of the connections were similar to sighted controls, there were two notable differences. The first is that S1 in bilateral enucleates received novel cortical inputs, that were not observed in sighted animals (e.g. CT). The second is that the density of inputs from some cortical fields that also projected to S1 in sighted controls were different in bilateral enucleates (e.g. piriform cortex and multimodal cortex). Two examples are shown; one in which an injection was restricted to the lateral portion of S1, further from the midline (Figure 4a) which represents the face, and one in which an injection was restricted to the portion of S1 closer to the midline (Figure 5), which represents the limbs and body. Neurons from a number of areas of the neocortex project to S1 in enucleates, with strong intrinsic projections from S1 (30.8%) and other somatosensory areas such as S2 (13.8%). Multimodal cortex (MM) also projected densely to S1 (16.4%), as did entorhinal and piriform cortex EC/Pir (10.3%; Table 3). S1 received moderate projections from the caudal SC (5.3%) and rostral SR (6.5%) somatosensory areas, from frontal cortex FM (3.5%), and A1 (4.0%). Finally, S1 received weak projections from caudotemporal cortex, CT (2.6%) and V1 (0.9%). For comparison, an injection into S1 of a sighted opossum (adapted from Dooley et al., 2013) is also provided in Figure 4a. In sighted opossums, the majority of projections to S1 are from within S1 (72.6%), with the only other notable projections originating from S2 (4.8%), SC (3.9%), and FM (10.6%).

Thus, comparisons with sighted opossums highlight novel and significantly different projections from A1 and CT, along with a significant increase in projections from S2, MM, and EC/Pir (Table 3; Figure 6a). This connectivity with CT is particularly notable, as CT in sighted opossums is densely connected with visual cortex (Kahn et al., 2000) and does not project to any parietal or frontal cortical areas (Dooley et al., 2013).

Thalamocortical connections of S1 in enucleates

As with the corticocortical projections to S1, a summary of the count and percentage of labeled cell bodies from each thalamic nuclei can be found in Table 4. Comparisons with sighted opossums (Dooley et al., 2014) revealed that there were differences in thalamocortical connections in enucleates and sighted opossums, but that these were subtler than differences in cortical connections. In bilateral enucleates, the strongest projections were from the ventral posterior nucleus VP (37.0%), as in sighted animals. Additional strong projections were from the posterior nuclei Pom/Pol (20.7%) and from the ventromedial nucleus VM (15.3%). As in sighted opossums (Dooley et al., 2014), projections from VP to S1 were largely from VPl when injections were localized to the medial portion of S1 (Figure $7a_6$-a_9) and from VPm when injections were localized to the lateral portion of S1 (Figure $8a_6$-a_{10}). S1 received moderate projections from the ventrolateral and ventroanterior nucleus (VL/VA; 12.5%), and weak and projections from MD (2.1%), VMb (1.9%), LGd (0.9%), and Pul (2.1%). Notably, the moderate projections from VL/VA (traditionally thalamic nuclei associated with the motor system) were consistent across all cases (see Figure $7a_1$-a_5 and Figure $8a_1$-a_5). Further, while thalamic projections from Pom/Pol to S1 in sighted animals were largely restricted to neurons dorsal to VP, enucleates also had moderate but consistent projections from Pom/Pol lateral to VP in all cases (Figure $7a_6$-a_9 and Figure $8a_6$-a_{10}).

In sighted short-tailed opossums, thalamic projections to S1 are largely restricted to VP and Pom, with nearly 80% of thalamic projections originating from these nuclei (Figure 6b; Dooley et al., 2014). In contrast, less than 60% of projections originate from VP and Pom/Pol in enucleates. Projections from Pom/Pol are not as topographically restricted in enucleates, with neurons lateral to VP in Pom/Pol appearing in all cases, a pattern never observed in sighted opossums (Dooley et al., 2014). Consistent with the small number of projections to S1 from primary cortical areas, less than 1% of cells projected from nuclei associated with visual and auditory processing to S1 (LGd and MGN, respectively). Instead, there was a significant increase in the projections from nuclei associated with the motor system (VL/VA) or other nuclei associated with somatosensory processing (VM). Further, unlike in sighted animals, projections from VL/VA and VM were consistently present in every animal.

Determination of Cortical Field Boundaries and Thalamic Nuclei

In order to identify the location of labeled cells following injections of anatomical tracers and to quantify the strength of connectivity from different cortical fields and thalamic nuclei to S1, it is critical to accurately and consistently define these structures across animals. In both bilaterally enucleated and sighted opossums, primary sensory areas (S1, A1 and V1) are easily defined as darkly stained regions of cortex in both myelin and parvalbumin (PV)

stained tissue (Figure 9; see Dooley et al., 2013; Karlen et al., 2006; Karlen & Krubitzer, 2009; Wong & Kaas, 2009). While we illustrate single sections of the cortex, the boundaries we show in our comprehensive reconstructions (Figure 4, Figure 5) are taken from an entire series of sections, as all cortical field boundaries are not always visible on a single section. The primary difference in cortical fields defined histologically between sighted and enucleated opossums is the reduction in size of V1 and the increase in size of S1, consistent with previous findings (Figure 1, Figure 9b, D; Karlen & Krubitzer, 2009). In myelin and PV stained tissue, SR and SC are thin moderately staining bands rostral and caudal to S1, respectively. MM is a lightly staining area between SC rostrally and visual cortex caudally. However, in general the more lateral portions of MM stained more darkly in enucleates compared to sighted opossums (compare cortex rostral to V1 in Figure 9b, d). CT stains darkly in both PV and myelin stained tissue in the most caudal and lateral portions of the neocortex.

At the level of the thalamus, in enucleates the optic tract is no longer present (Figure 9a, c, e, g), and in tissue stained for vGluT2 and PV, LGd and LGv are lighter than surrounding nuclei (compare 9c and e to 9d and f). However, the boundaries of these visual nuclei could be identified in CO sections, and as quantified in earlier studies, LGd and LGv are reduced in size compared to sighted animals (Karlen & Krubitzer, 2009). Similar findings have been reported for the LGd of enucleated rats (Fujiyama et al., 2003; Hada et al., 1999). The pulvinar, another visual nucleus, also stains lighter in enucleates compared to sighted animals, but still appeared darker than adjacent nuclei in CO and PV stained tissue (Figure 10a, e). Notably, visual thalamic nuclei of enucleates lack internal structure seen in sighted animals (α and β sublaminae in LGd, Olkowicz et al., 2008; lateral portion of LGv; and the caudal subdivision of the pulvinar, Dooley et al., 2014). Nuclei in the ventral nuclear complex (including VM, VMb, and VP) were readily identified in P4 enucleates, staining more darkly than surrounding laminae and nuclei. The boundaries between VL and VA could not be identified in all sections, so these nuclei were grouped together as VL/VA. This was also true for Pom and Pol, which we grouped together as Pom/Pol. Retrogradely labeled cells that could not be confidently attributed to a specific thalamic nucleus, and nuclei which did not have enough labeled cells to be counted as weakly connected, were classified as "other."

Discussion:

The goal of this study was to examine and quantify the effects of early bilateral enucleation on corticocortical and thalamocortical connections of the primary somatosensory cortex (S1) in short-tailed opossums and to compare these to connections of S1 in sighted opossums (Dooley et al., 2013, 2014). The present investigation was prompted by the finding that following very early enucleation, the primary somatosensory cortex increases in size (Karlen et al., 2006), neurons in S1 respond to both somatosensory and auditory stimulation (Kahn & Krubitzer, 2002; Karlen et al., 2006) and the neural response properties and receptive field size are altered compared to sighted controls (Ramamurthy & Krubitzer, 2018; Figure 1). Here, we provide anatomical evidence for both novel corticocortical projections, as well as changes in the density of existing corticocortical and thalamocortical projections to S1 resulting from early loss of vision (Figure 11a).

While there are many studies that examine cross modal changes to multimodal areas following loss of, or alterations in, sensory inputs (Bavelier & Neville, 2002; Lomber et al., 2010; Meredith et al., 2016), this is the first study to quantify changes in cortical and subcortical connectivity of a primary sensory area associated with a spared sensory system. Our findings demonstrate that cortical and subcortical connections of the developing brain are highly dependent on the ratio of incoming inputs from different sensory receptor arrays. We experimentally altered the ratio of sensory inputs by completely removing all visual input, thereby reweighting auditory, somatosensory, gustatory and olfactory inputs in the developing nervous system. This type of reweighting occurs naturally, as evidenced in highly specialized mammals such as echolocating bats. In these mammals the entire auditory pathway has been elaborated and visual pathways have been reduced, and the amount of cortex devoted to processing auditory inputs is greatly expanded (Esser et al., 1999; Hoffmann et al., 2008). While the effect of changing the ratio of incoming sensory inputs are readily determined in our experimental paradigm as well as in mammals with extreme specialization, we propose that all developing brains are exposed to different combinations of sensory input due to both specialization of their sensory systems and to the environmental context in which the brain develops.

The opossum is one of the few animal models where enucleations can be performed *ex-utero* prior to retinal ganglion cell axons reaching their thalamic targets (Figure 2). Since most of the studies that examine the effects of loss of visual input performed enucleations at a later developmental stage than the current study (i.e. after the formation of thalamocortical connections) there are only a few studies with which the present study can be directly compared. These include bilateral enucleations in fetal macaque monkeys (e.g. Dehay et al., 1989, 1991; Rakic et al., 1991), and anophthalmic (eyeless) mice (Chabot et al., 2008; Chabot et al., 2007; Charbonneau et al., 2012). For opossums and macaques, enucleations occurred before visual pathways were established, and for anophthalmic mice, the eyes were never present. Common to all of these investigations, V1 decreased in size, and in opossums and anophthalmic mice, somatosensory cortex increased in size (Karlen & Krubitzer, 2009; Masse et al., 2014). Further, all of these studies document abnormalities in the connections of V1, with opossums and anophthalmic mice having cortical projections to V1 from structures associated with processing inputs from the somatosensory and auditory systems (Charbonneau et al., 2012; Karlen et al., 2006). Surprisingly, other than the present investigation there are no other studies that examine the anatomical consequences of early loss of vision (before the retinal ganglion axons reach their targets) on primary somatosensory or auditory cortex (e.g. S1 or A1), or even secondary fields (e.g. S2 or R). Further, other than studies of the functional organization of S1 in bilaterally enucleated opossums from our own laboratory, there is only one other study that provides any evidence, through an indirect measure of neural activity, for functional changes in S1 following early loss of vision. This is a study in mice that were bilaterally enucleated at birth. In these animals, larger sized barrels were observed in S1 compared to unmanipulated controls (Rauschecker et al., 1992).

At what level are connections altered?

The current investigation focuses on corticocortical and thalamocortical connections that are altered when input is lost prior to the formation of retinofugal and geniculocortical pathways. However, there is also evidence that cross-modal alterations may occur at very early levels of processing. In mice and cats that were visually deprived on the day of birth, the vibrissae had an increased diameter and length (Rauschecker et al., 1992), suggesting that loss of inputs from one sensory system may affect the peripheral morphology of the sensory receptor arrays of the spared systems, and thus their transduction properties. Previous studies in anophthalmic mice indicate that alterations in connectivity can occur throughout the entire brain, from the brainstem to the cortex. In eyeless mice, the LGd receives input from the inferior colliculus, a structure normally associated with auditory processing (Chabot et al., 2008; Chabot et al., 2007) as well as the dorsal column nuclei, brainstem nuclei normally associated with the somatosensory system (Asanuma & Stanfield, 1990). Thus, the cross-modal changes of experimental manipulations in which visual input is absent or lost at the earliest stages of development are consistent with those observed naturally in evolution when vision is lost.

Similar subcortical plasticity has been shown for the auditory system. For example, in mice that are congenitally deaf due to anatomical and functional abnormalities in the cochlea, retinal ganglion cells project not only to their normal thalamic targets (the LGd and the pulvinar), but also to divisions of the medial geniculate nucleus (Hunt et al., 2006). In early deafened ferrets and cats, neurons in auditory core areas respond to somatosensory stimulation, but these changes in functional organization were not accompanied by alterations in cortical connectivity of the primary or higher order auditory areas (Meredith and Lomber, 2011; Meredith and Allman, 2012), but were likely the result of changes at subcortical levels such as the cochlear nucleus. It should be noted that ferrets in that study were deafened at P49 which is after the formation of thalamocortical (P1; Herrmannet al, 1994) and corticocortical (P45; Durack and Katz, 1996) connections, indicating that the age at which the loss occurs, as well as the species examined are critical factors that determine the location and extent of anatomical changes.

Implications for gene targeted therapies and retinal prosthetics

When asked to imagine what it is like to be blind, most individuals start by closing their eyes. However, given the dramatic cross-modal alterations in connectivity at all levels of the nervous system it is clear that blindness is not simply an absence of light. And as discussed above, blindness (especially early blindness) affects the entire nervous system. Thus, simply restoring vision later in life would not result in "seeing" in the same manner as individuals who developed with normal visual input. Whereas most modern therapeutic interventions such as gene-targeted therapies and retinal prosthetics focus on the eye (Caspi et al., 2017; Liu et al., 2012; Lorach et al., 2013; Santos-Ferreira et al., 2016, see Fine et al., 2015 for review) recent studies demonstrate that restoration of retinal function later in life following years of visual deprivation or early loss does not fully restore vision, and individuals have deficits in object and face recognition (Fine et al., 2003), shape recognition (McKyton et al., 2015) and parsing (Ostrovsky et al., 2009) to name a few. This is not surprising given the radical alterations in connectivity that occur at all levels of processing, and the plethora of

studies that underscore the importance of early visual experience for the development of a number of fundamental properties of neurons in the visual cortex, including direction selectivity (Ye Li et al., 2006; Ye Li et al., 2008), orientation selectivity (White et al., 2001) and binocular vision (Sarnaik et al., 2014; see White & Fitzpatrick, 2007 for review).

Clearly the effectiveness of the therapies described above relies on the age of blindness onset, severity of the impairment as well as the age of therapeutic/rehabilitative intervention. Results from the present study, as well as previous studies which examine the effects of early loss of vision (and in one case auditory enhancement; Piche et al., 2004), indicate that individuals may be better served by therapeutic strategies that harness and direct the naturally occurring functional and anatomical plasticity of the neocortex, and other subcortical pathways, by providing therapies that augment the spared sensory systems.

Acknowledgements

Abbreviations

Cortical Areas

A1	Primary auditory cortex
CT	Caudal temporal area
EC	Entorhinal cortex
FM	Frontal myelinated area
MM	Multimodal cortex
Pir	Piriform cortex
S1	Primary somatosensory cortex
S2	Second somatosensory cortex
SC	Somatosensory caudal area
SR	Somatosensory rostral area
V1	Primary visual cortex
V2	Second visual cortex

Subcortical structures

APT	Anterior pretectum
Hb	Habenula
LGd	Lateral geniculate nucleus, dorsal division

LGv	Lateral geniculate nucleus, ventral division
MD	Medial dorsal nucleus
MGN	Medial geniculate nucleus
mt	Mammillothalamic tract
MV	Medioventral nucleus
MV	Medioventral nucleus
ot	Optic tract
PF	Parafascicular nucleus
Pol	Posterior nucleus (lateral)
Pom	Posterior nucleus (medial)
Pul	Pulvinar
VA	Ventral anterior nucleus
VL	Ventrolateral nucleus
VM	Ventromedial nucleus
VMb	Ventral medial basal nucleus
VP	Ventral posterior nucleus
VPl	Ventral posterior lateral nucleus
VPm	Ventral posterior medial nucleus

Other abbreviations

CO	Cytochrome oxidase
CTB	Cholera toxin subunit-B
FE	Fluoro-ruby
FR	Fluoro-emerald
PV	Parvalbumin
vGluT2	Vesicular glutamate transporter 2

References

Abbott CW, Kozanian O, and Huffman KJ (2015). The effects of lifelong blindness on murine neuroanatomy and gene expression. Front in Aging Neurosci, 7:144. doi: 10.3389/fnagi.2015.00144

Arnott SR, Thaler L, Milne JL, Kish D, & Goodale MA (2013). Shape-specific activation of occipital cortex in an early blind echolocation expert. Neuropsychologia, 51(5), 938–949. doi:10.1016/j.neuropsychologia.2013.01.024 [PubMed: 23391560]

Asanuma C, & Stanfield BB (1990). Induction of somatic sensory inputs to the lateral geniculate nucleus in congenitally blind mice and in phenotypically normal mice. Neuroscience, 39(3), 533–545. [PubMed: 1711167]

Bavelier D, & Neville HJ (2002). Cross-modal plasticity: where and how? Nat Rev Neurosci, 3(6), 443–452. doi:10.1038/nrn848 [PubMed: 12042879]

Bedny M, Richardson H, & Saxe R (2015). "Visual" Cortex Responds to Spoken Language in Blind Children. J Neurosci, 35(33), 11674–11681. doi:10.1523/JNEUROSCI.0634-15.2015 [PubMed: 26290244]

Bhattacharjee A, Ye AJ, Lisak JA, Vargas MG, & Goldreich D (2010). Vibrotactile masking experiments reveal accelerated somatosensory processing in congenitally blind braille readers. J Neurosci, 30(43), 14288–14298. doi:10.1523/JNEUROSCI.1447-10.2010 [PubMed: 20980584]

Butler BE, Chabot N, Kral A, Lomber SG (2017). Origins of thalamic and cortical projections to the posterior auditory field in congenitally deaf cats. Hear Res, 343:118–127. doi:10.1016/j.heares.2016.06.003 [PubMed: 27306930]

Caspi A, Roy A, Dorn JD, & Greenberg RJ (2017). Retinotopic to Spatiotopic Mapping in Blind Patients Implanted With the Argus II Retinal Prosthesis. Invest Ophthalmol Vis Sci, 58(1), 119–127. doi:10.1167/iovs.16-20398 [PubMed: 28114567]

Chabot N, Charbonneau V, Laramee ME, Tremblay R, Boire D, & Bronchti G (2008). Subcortical auditory input to the primary visual cortex in anophthalmic mice. Neurosci Lett, 433(2), 129–134. doi:10.1016/j.neulet.2008.01.003 [PubMed: 18276073]

Chabot N, Robert S, Tremblay R, Miceli D, Boire D, & Bronchti G (2007). Audition differently activates the visual system in neonatally enucleated mice compared with anophthalmic mutants. Eur J Neurosci, 26(8), 2334–2348. doi:10.1111/j.1460-9568.2007.05854.x [PubMed: 17953622]

Charbonneau V, Laramee ME, Boucher V, Bronchti G, & Boire D (2012). Cortical and subcortical projections to primary visual cortex in anophthalmic, enucleated and sighted mice. Eur J Neurosci, 36(7), 2949–2963. doi:10.1111/j.1460-9568.2012.08215.x [PubMed: 22780435]

Dehay C, Horsburgh G, Berland M, Killackey H, & Kennedy H (1989). Maturation and connectivity of the visual cortex in monkey is altered by prenatal removal of retinal input. Nature, 337(6204), 265–267. doi:10.1038/337265a0 [PubMed: 2536139]

Dehay C, Horsburgh G, Berland M, Killackey H, & Kennedy H (1991). The effects of bilateral enucleation in the primate fetus on the parcellation of visual cortex. Brain Res Dev Brain Res, 62(1), 137–141. [PubMed: 1760867]

Djavadian R, Bisti S, Maccarone R, Bartkowska K, & Turlejski K (2006). Development and plasticity of the retina in the opossum Monodelphis domestica. Acta Neurobiol Exp (Wars), 66(3), 179–188. [PubMed: 17133949]

Dooley JC, Franca JG, Seelke AM, Cooke DF, & Krubitzer LA (2013). A connection to the past: Monodelphis domestica provides insight into the organization and connectivity of the brains of early mammals. J Comp Neurol, 521(17), 3877–3897. doi:10.1002/cne.23383 [PubMed: 23784751]

Dooley JC, Franca JG, Seelke AM, Cooke DF, & Krubitzer LA (2014). Evolution of mammalian sensorimotor cortex: thalamic projections to parietal cortical areas in Monodelphis domestica. Front Neuroanat, 8, 163. doi:10.3389/fnana.2014.00163 [PubMed: 25620915]

Durack JC & Katz LC Development of horizontal projections in layer 2/3 of ferret visual cortex. Cereb Cortex. 6(2):178–83. [PubMed: 8670648]

Esser KH and Eiermann A, Tonotopic organization and parcellation of auditory cortex in the FM-bat Carollia perspicillata. Eur J Neurosci, 1999 11(10): p. 3669–3682. [PubMed: 10564374]

Fine I, Cepko CL, & Landy MS (2015). Vision research special issue: Sight restoration: Prosthetics, optogenetics and gene therapy. Vision Res, 111(Pt B), 115–123. doi:10.1016/j.visres.2015.04.012 [PubMed: 25937376]

Fine I, Wade AR, Brewer AA, May MG, Goodman DF, Boynton GM, … MacLeod DI (2003). Long-term deprivation affects visual perception and cortex. Nat Neurosci, 6(9), 915–916. doi:10.1038/nn1102 [PubMed: 12937420]

Fujiyama F, Hioki H, Tomioka R, Taki K, Tamamaki N, Nomura S, … Kaneko T (2003). Changes of immunocytochemical localization of vesicular glutamate transporters in the rat visual system after

the retinofugal denervation. J Comp Neurol, 465(2), 234–249. doi:10.1002/cne.10848 [PubMed: 12949784]

Gallyas F (1979). Silver staining of myelin by means of physical development. Neurol Res. (2):203–9. [PubMed: 95356]

Gizewski ER, Gasser T, de Greiff A, Boehm A, & Forsting M (2003). Cross-modal plasticity for sensory and motor activation patterns in blind subjects. Neuroimage, 19(3), 968–975. [PubMed: 12880825]

Gougoux F, Zatorre RJ, Lassonde M, Voss P, & Lepore F (2005). A functional neuroimaging study of sound localization: visual cortex activity predicts performance in early-blind individuals. PLoS Biol, 3(2), e27. doi:10.1371/journal.pbio.0030027 [PubMed: 15678166]

Hada Y, Yamada Y, Imamura K, Mataga N, Watanabe Y, & Yamamoto M (1999). Effects of monocular enucleation on parvalbumin in rat visual system during postnatal development. Invest Ophthalmol Vis Sci, 40(11), 2535–2545. [PubMed: 10509647]

Henschke JU, Oelschlegel AM, Angenstein F, Ohl FW, Goldschmidt J, Kanold PO, Budinger E (2018). Early sensory experience influences the development of multisensory thalamocortical and intracortical connections of primary sensory cortices. Brain Struct Funct. 233:1165–1190.

Herrmann K, Antonini A, & Shatz CJ (1994). Ultrastructural evidence for synaptic interactions between thalamocortical axons and subplate neurons. Eur J Neurosci. 6(11):1729–42. [PubMed: 7874312]

Hoffmann S, Firzlaff U, Radtke-Schuller S, Schwellnus B, and Schuller G (2008). The auditory cortex of the bat Phyllostomus discolor: Localization and organization of basic response properties. BMC Neurosci, 9:65. [PubMed: 18625034]

Hunt DL, Yamoah EN, & Krubitzer L (2006). Multisensory plasticity in congenitally deaf mice: how are cortical areas functionally specified? Neuroscience, 139(4), 1507–1524. doi:10.1016/j.neuroscience.2006.01.023 [PubMed: 16529873]

Kahn DM, Huffman KJ, & Krubitzer L (2000). Organization and connections of V1 in Monodelphis domestica. The Journal of Comparative Neurology, 428(2), 337–354. [PubMed: 11064371]

Kahn DM, & Krubitzer L (2002). Massive cross-modal cortical plasticity and the emergence of a new cortical area in developmentally blind mammals. Proceedings of the National Academy of Sciences of the United States of America, 99(17), 11429–11434. doi:10.1073/pnas.162342799 [PubMed: 12163645]

Karlen SJ, Kahn DM, & Krubitzer L (2006). Early blindness results in abnormal corticocortical and thalamocortical connections. Neuroscience, 142(3), 843–858. doi:10.1016/j.neuroscience.2006.06.055 [PubMed: 16934941]

Karlen SJ, & Krubitzer L (2009). Effects of bilateral enucleation on the size of visual and nonvisual areas of the brain. Cereb Cortex, 19(6), 1360–1371. doi:10.1093/cercor/bhn176 [PubMed: 18842663]

Kolarik AJ, Scarfe AC, Moore BC, & Pardhan S (2017). Blindness enhances auditory obstacle circumvention: Assessing echolocation, sensory substitution, and visual-based navigation. PLoS One, 12(4), e0175750. doi:10.1371/journal.pone.0175750 [PubMed: 28407000]

Lewald J (2013). Exceptional ability of blind humans to hear sound motion: implications for the emergence of auditory space. Neuropsychologia, 51(1), 181–186. doi:10.1016/j.neuropsychologia.2012.11.017 [PubMed: 23178211]

Li Y, Fitzpatrick D, & White LE (2006). The development of direction selectivity in ferret visual cortex requires early visual experience. Nature Neuroscience, 9(5), 676–681. doi:10.1038/nn1684 [PubMed: 16604068]

Li Y, Van Hooser SD, Mazurek M, White LE, & Fitzpatrick D (2008). Experience with moving visual stimuli drives the early development of cortical direction selectivity. Nature, 456(7224), 952–956. doi:10.1038/nature07417 [PubMed: 18946471]

Liu Y, Tang L, & Chen B (2012). Effects of antioxidant gene therapy on retinal neurons and oxidative stress in a model of retinal ischemia/reperfusion. Free Radic Biol Med, 52(5), 909–915. doi:10.1016/j.freeradbiomed.2011.12.013 [PubMed: 22240151]

Lomber SG, Meredith MA, & Kral A (2010). Cross-modal plasticity in specific auditory cortices underlies visual compensations in the deaf. Nat Neurosci, 13(11), 1421–1427. doi:10.1038/nn. 2653 [PubMed: 20935644]

Lorach H, Marre O, Sahel JA, Benosman R, & Picaud S (2013). Neural stimulation for visual rehabilitation: advances and challenges. J Physiol Paris, 107(5), 421–431. doi:10.1016/j.jphysparis.2012.10.003 [PubMed: 23148976]

Masse IO, Guillemette S, Laramee ME, Bronchti G, & Boire D (2014). Strain differences of the effect of enucleation and anophthalmia on the size and growth of sensory cortices in mice. Brain Res, 1588, 113–126. doi:10.1016/j.brainres.2014.09.025 [PubMed: 25242615]

McKyton A, Ben-Zion I, Doron R, & Zohary E (2015). The Limits of Shape Recognition following Late Emergence from Blindness. Curr Biol, 25(18), 2373–2378. doi:10.1016/j.cub.2015.06.040 [PubMed: 26299519]

Meredith MA & Allman BL (2012). Early Hearing-Impairment Results in Crossmodal Reorganization of Ferret Core Auditory Cortex. Neuro. Plas. doi:10.1155/2012/601591

Meredith MA & Lomber SG (2011). Somatosensory and visual crossmodal plasticity in the anterior auditory field of early-deaf cats. Hear Res. 280(1–2):38–47. doi: 10.1016/j.heares.2011.02.004 [PubMed: 21354286]

Meredith MA, Clemo HR, Corley SB, Chabot N, & Lomber SG (2016). Cortical and thalamic connectivity of the auditory anterior ectosylvian cortex of early-deaf cats: Implications for neural mechanisms of crossmodal plasticity. Hear Res, 333, 25–36. doi:10.1016/j.heares.2015.12.007 [PubMed: 26724756]

Molnár Z, Knott GW, Blakemore C, & Saunders NR (1998). Development of thalamocortical projections in the South American gray short-tailed opossum (Monodelphis domestica). The Journal of Comparative Neurology, 398(4), 491–514. [PubMed: 9717705]

Norman JF, & Bartholomew AN (2011). Blindness enhances tactile acuity and haptic 3-D shape discrimination. Atten Percept Psychophys, 73(7), 2323–2331. doi:10.3758/s13414-011-0160-4 [PubMed: 21671153]

Olkowicz S, Turlejski K, Bartkowska K, Wielkopolska E, & Djavadian RL (2008). Thalamic nuclei in the opossum Monodelphis domestica. J Chem Neuroanat, 36(2), 85–97. doi:10.1016/j.jchemneu.2008.05.003 [PubMed: 18571895]

Ostrovsky Y, Meyers E, Ganesh S, Mathur U, & Sinha P (2009). Visual parsing after recovery from blindness. Psychol Sci, 20(12), 1484–1491. doi:10.1111/j.1467-9280.2009.02471.x [PubMed: 19891751]

Piche M, Robert S, Miceli D, & Bronchti G (2004). Environmental enrichment enhances auditory takeover of the occipital cortex in anophthalmic mice. Eur J Neurosci, 20(12), 3463–3472. doi:10.1111/j.1460-9568.2004.03823.x [PubMed: 15610179]

Rakic P, Suner I, & Williams RW (1991). A novel cytoarchitectonic area induced experimentally within the primate visual cortex. Proc Natl Acad Sci U S A, 88(6), 2083–2087. [PubMed: 2006147]

Ramamurthy DL, & Krubitzer LA (2018). Neural coding of whisker-mediated touch in primary somatosensory cortex is altered following early blindness. J Neuro, doi: 10.1523/jneurosci. 0066-18.2018

Rauschecker JP, Tian B, Korte M, & Egert U (1992). Crossmodal changes in the somatosensory vibrissa/barrel system of visually deprived animals. Proc Natl Acad Sci U S A, 89(11), 5063–5067. [PubMed: 1594614]

Ricciardi E, Handjaras G, & Pietrini P (2014). The blind brain: how (lack of) vision shapes the morphological and functional architecture of the human brain. Exp Biol Med (Maywood), 239(11), 1414–1420. doi:10.1177/1535370214538740 [PubMed: 24962172]

Sakaguchi DS, Hoffelen SV, Greenlee MHW, Harper MM, & Au DT (2008). Cell birth and death in the developing retina of the Brazilian opossum, Monodelphis domestica. Brain Research, 1195, 28–42. doi:10.1016/j.brainres.2007.12.018 [PubMed: 18191114]

Santos-Ferreira T, Llonch S, Borsch O, Postel K, Haas J, & Ader M (2016). Retinal transplantation of photoreceptors results in donor-host cytoplasmic exchange. Nat Commun, 7, 13028. doi:10.1038/ncomms13028 [PubMed: 27701381]

Sarnaik R, Wang BS, & Cang J (2014). Experience-dependent and independent binocular correspondence of receptive field subregions in mouse visual cortex. Cereb Cortex, 24(6), 1658–1670. doi:10.1093/cercor/bht027 [PubMed: 23389996]

Seelke AM, Dooley JC, & Krubitzer LA (2012). The emergence of somatotopic maps of the body in S1 in rats: the correspondence between functional and anatomical organization. PLoS One, 7. doi: 10.1371/journal.pone.0032322

Sieben K, Bieler M, Roder B, Hanganu-Opatz IL (2015). Neonatal Restriction of Tactile Inputs Leads to Long-Lasting Impairments of Cross-Modal Processing. Plos Bio. 13(11) e1002304. doi: 10.1371/journal.pbio.1002304 [PubMed: 26600123]

Slimani H, Ptito M, & Kupers R (2015). Enhanced heat discrimination in congenital blindness. Behav Brain Res, 283, 233–237. doi:10.1016/j.bbr.2015.01.037 [PubMed: 25639543]

Taylor JS, & Guillery RW (1994). Early development of the optic chiasm in the gray short-tailed opossum, Monodelphis domestica. The Journal of Comparative Neurology, 350(1), 109–121. doi: 10.1002/cne.903500108 [PubMed: 7860795]

Thaler L, & Goodale MA (2016). Echolocation in humans: an overview. Wiley Interdisc Rev Cogn Sci, 7(6), 382–393. doi:10.1002/wcs.1408 [PubMed: 27538733]

Vercillo T, Milne JL, Gori M, & Goodale MA (2015). Enhanced auditory spatial localization in blind echolocators. Neuropsychologia, 67, 35–40. doi:10.1016/j.neuropsychologia.2014.12.001 [PubMed: 25484307]

White LE, Coppola DM, & Fitzpatrick D (2001). The contribution of sensory experience to the maturation of orientation selectivity in ferret visual cortex. Nature, 411(6841), 1049–1052. doi: 10.1038/35082568 [PubMed: 11429605]

White LE, & Fitzpatrick D (2007). Vision and cortical map development. Neuron, 56(2), 327–338. doi: 10.1016/j.neuron.2007.10.011 [PubMed: 17964249]

Wong-Riley MTT (1989). Cytochrome oxidase: an endogenous metabolic marker for neuronal activity. Trends in Neurosciences, 12, 94–101. [PubMed: 2469224]

Wong P, & Kaas JH (2009). An architectonic study of the neocortex of the short-tailed opossum (Monodelphis domestica). Brain Behav Evol, 73(3), 206–228. doi:10.1159/000225381 [PubMed: 19546531]

We investigated whether early bilateral enucleation alters cortical and thalamic projections to S1. Following enucleation, S1 receives dense inputs from novel cortical fields, and that the density of existing cortical and thalamocortical connections was altered. Our results demonstrate that alterations in sensory input affect the organization of other sensory systems.
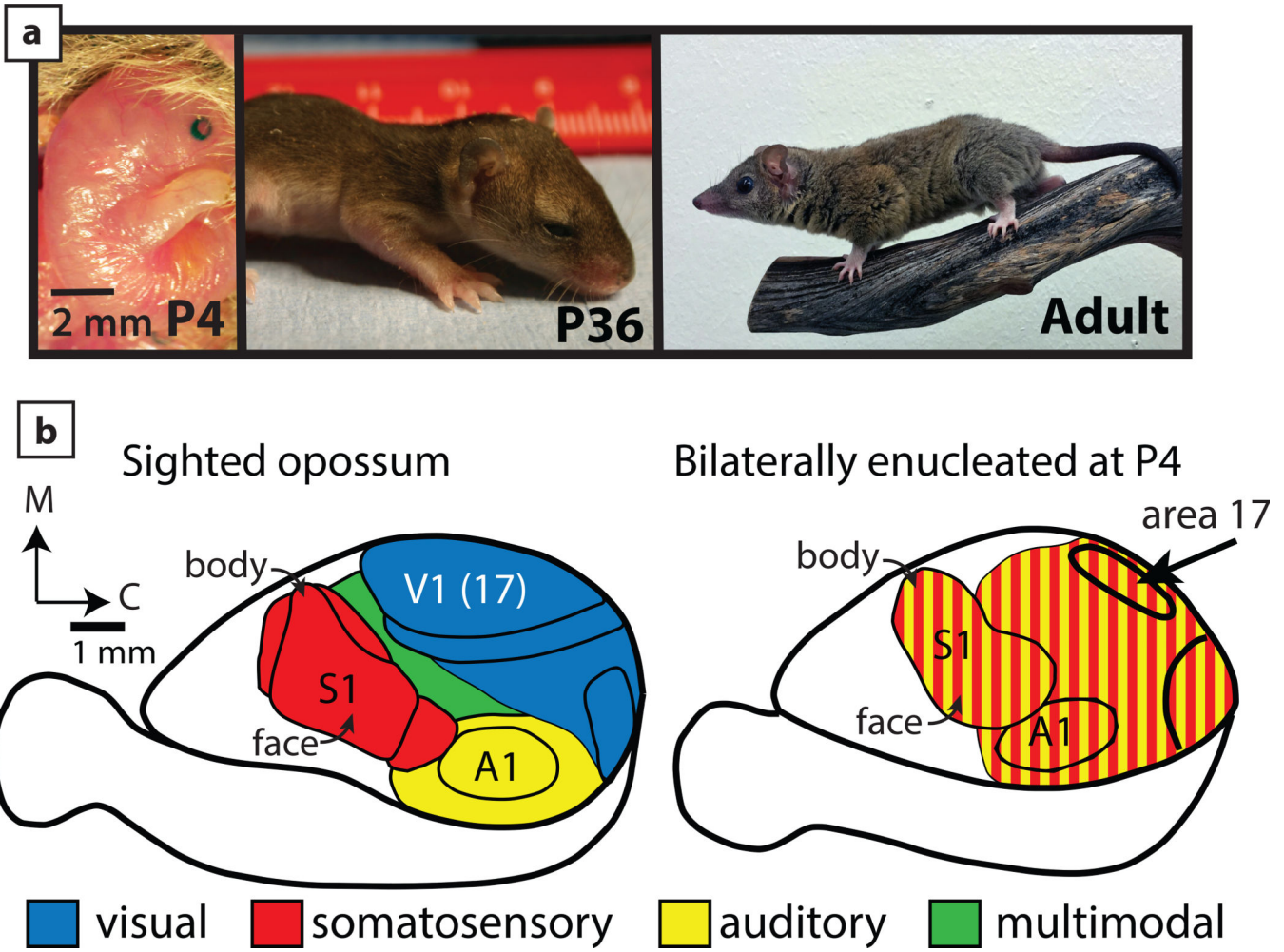
Figure 1:
(a) Photographs of sighted short-tailed opossums on the age of enucleation (left, P4), immediately following eye opening (middle, P36), and as adults (right). (b) In sighted opossums, much of cortex is devoted to visual processing (bottom left). In P4 bilateral enucleates, all of what would be visual cortex is taken over by the somatosensory and auditory system (bottom right). In most of the animals examined using neurophysiological mapping techniques, both auditory and somatosensory cortex were re-organized as well. Bottom figures are adapted from Kahn & Krubitzer, 2002; Karlen et al., 2006.
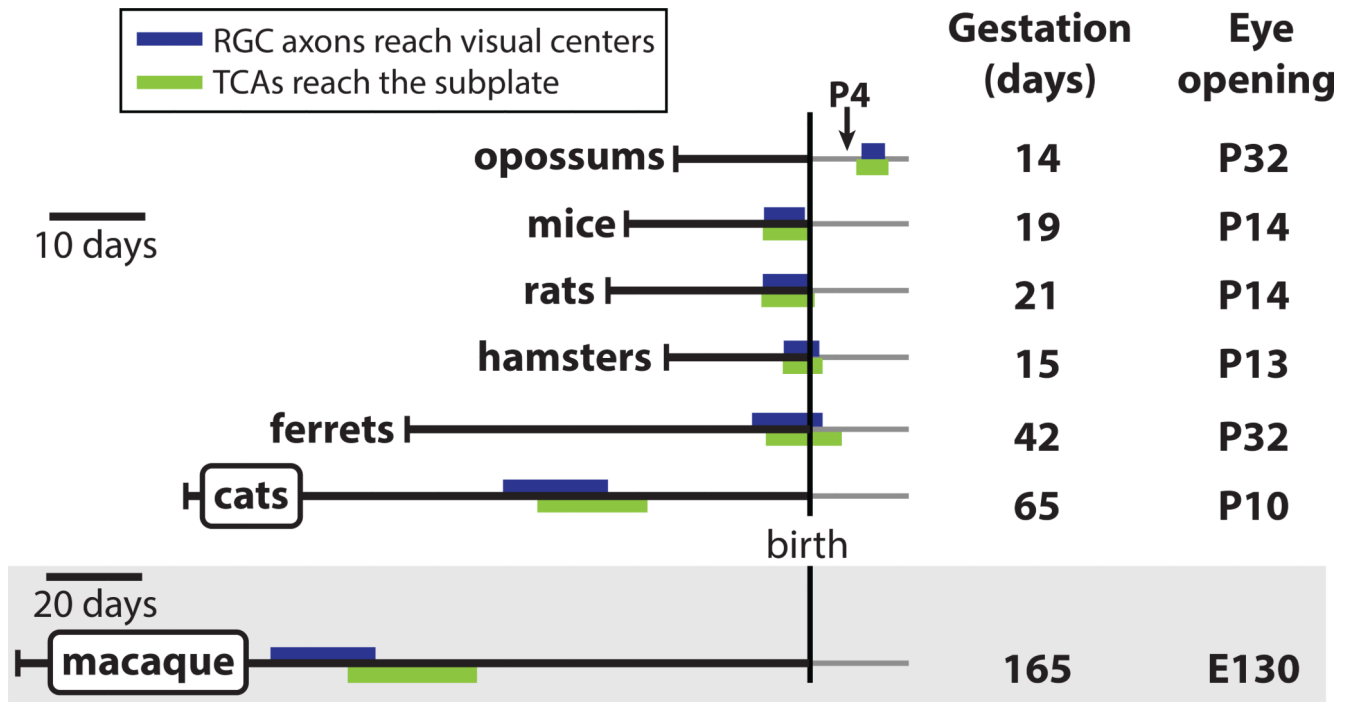
Figure 2:

The development of thalamocortical axons (TCAs) and retinal ganglion cell (RGC) axons in short-tailed opossums (*Monodelphis domestica*) compared to other species in which enucleations have been performed. Some of the major developmental milestones are shown relative to birth. At the time enucleations are made in the present study, thalamocortical afferents have yet to reach the cortex and retinal ganglion cell axons have yet to reach the diencephalon. Both of these events begin before birth in other species in enucleations were performed. Scale bar is the same for all species listed (10 days) except macaque (20 days).
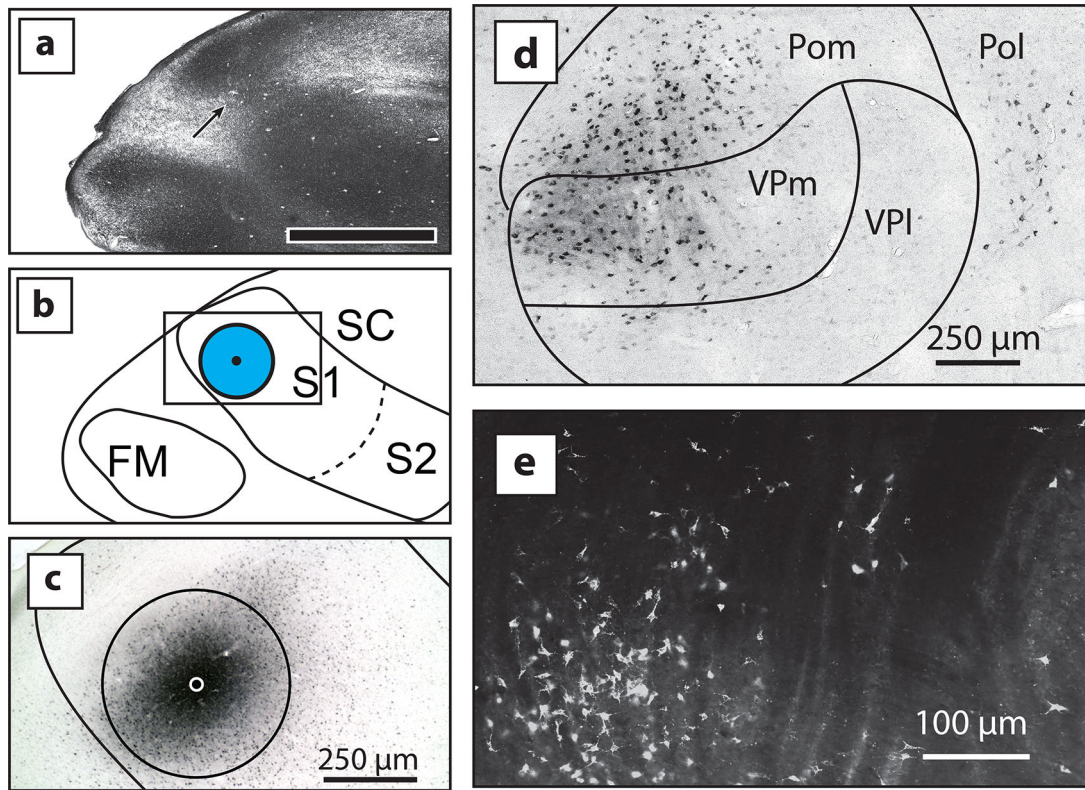
Figure 3:
Cortical injection site of S1 in a P4 enucleate. (a) Myelin stain showing injection site (arrow), along with cortical fields boundaries (b) determined from the entire series of myelin-stained sections. Scale bar in A is 1 mm. Injection site center and surrounding halo are shown as black dot and a blue circle respectively. (c) An enlarged image of the boxed area in image B showing tissue stained for CTB expression. This image shows the injection and halo of CTB. Scale bar = 250 um. (d) A thalamic section stained for CTB showing stained neurons in VPm and Pom (left) and Pol (right). Boundaries of thalamic nuclei are based on adjacent sections. (e) Thalamic cells in VA/VL stained for FR.
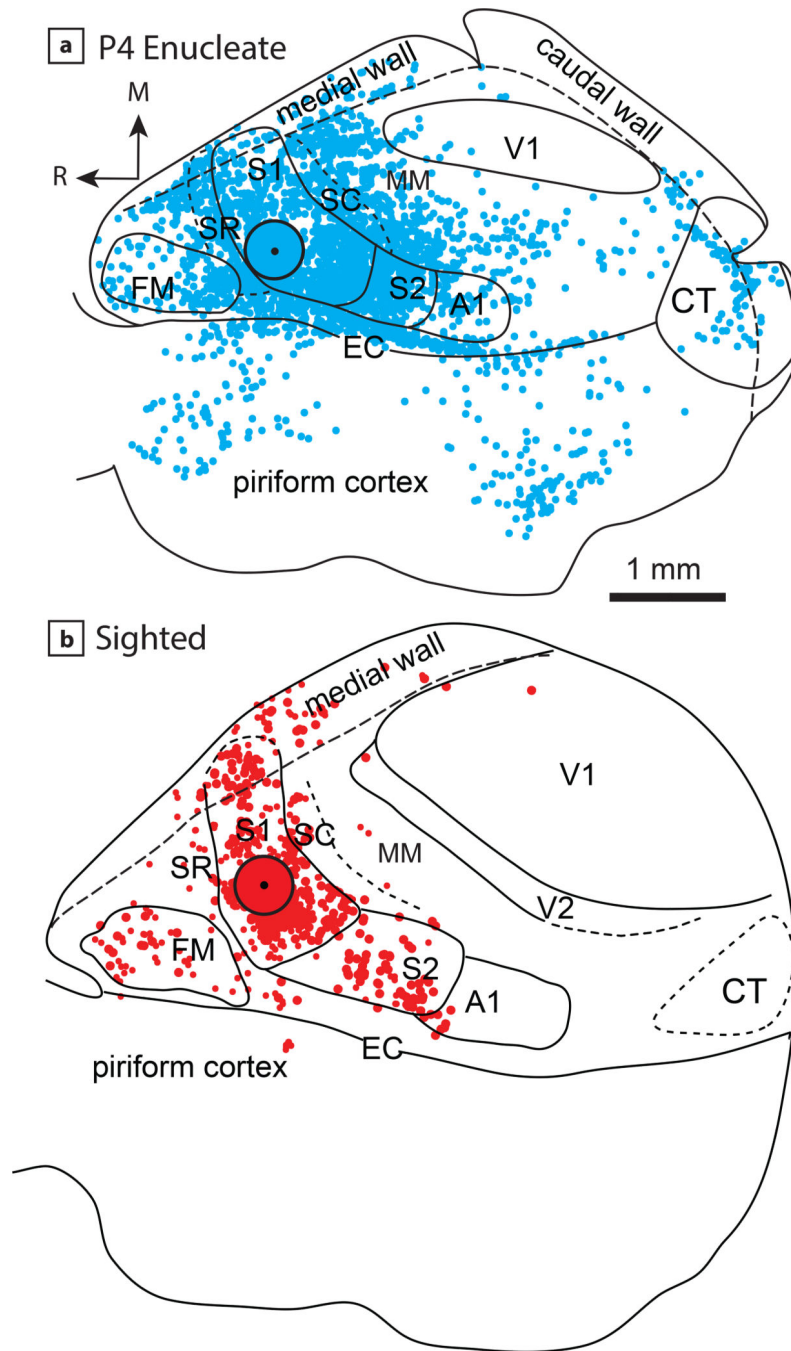
Figure 4:
Corticocortical connections of the lateral portion of S1 in a P4 enucleate (a) and sighted opossum (b). (a) Retrograde labeled cell bodies (blue dots) revealed from a CTB injection centered in the lateral (face) representation of S1, with neurons shown in S2, SC, SR, A1, EC/Pir and CT. (d) An FR injection in the face representation of S1 in a sighted opossum (adapted from Dooley et al., 2013), with retrograde labeled cell bodies (red dots) illustrated over anatomical boundaries. The sighted animal shows a much more restricted pattern of projections, with very few neurons projecting to S1 in cortical areas caudal to SC.
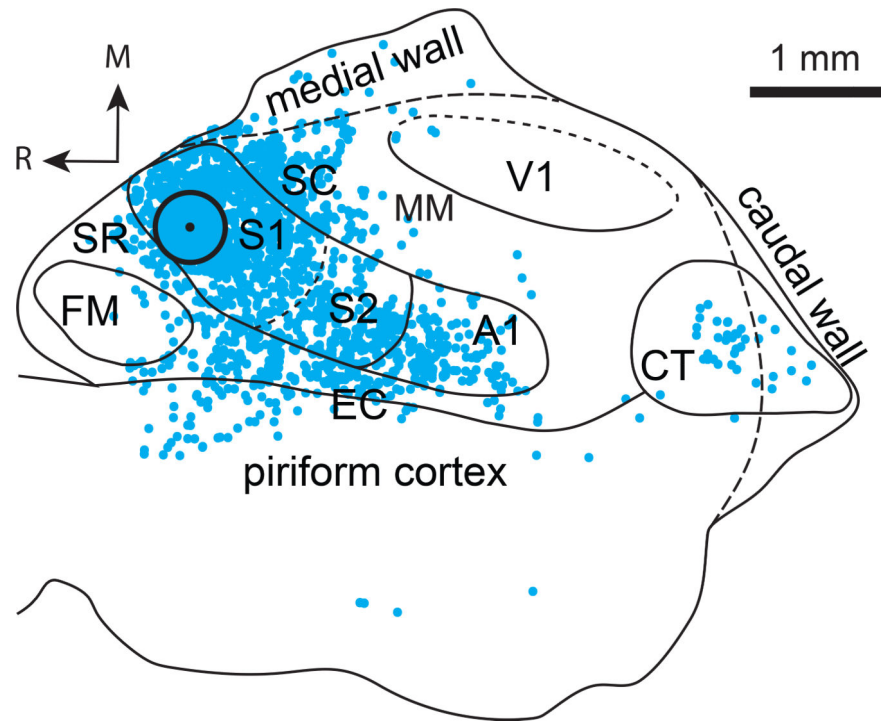
Figure 5:
An injection of CTB into medial S1, in the representation of the body, showing extensive
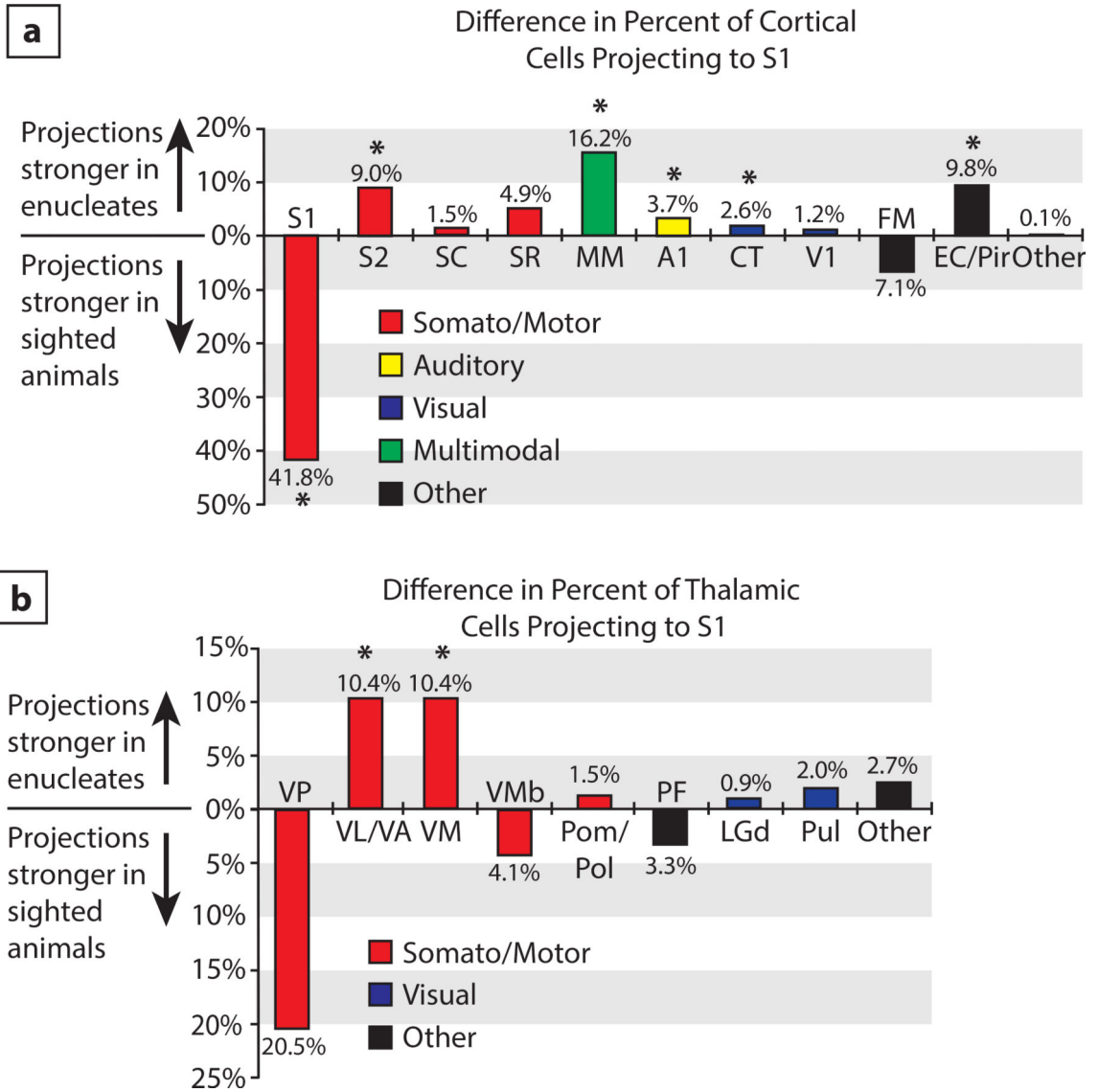projections from multiple areas of the neocortex. Conventions as in Figure 4.

Figure 6:

Comparison of (a) cortical and (b) thalamic projections to S1 between sighted opossums and opossums enucleated on P4. Bars represent the total percentage of connections (out of 100%) projecting from each area to the injection site in S1 of enucleated animals, minus the percentage found from that area in sighted opossums. Thus, a bar facing upwards represents a projection that is stronger in enucleates animals, and a bar facing downwards represents a projection that is stronger in sighted animals. Bars are colored by the sensory modality. Asterisks indicate significance ($P < 0.05$).
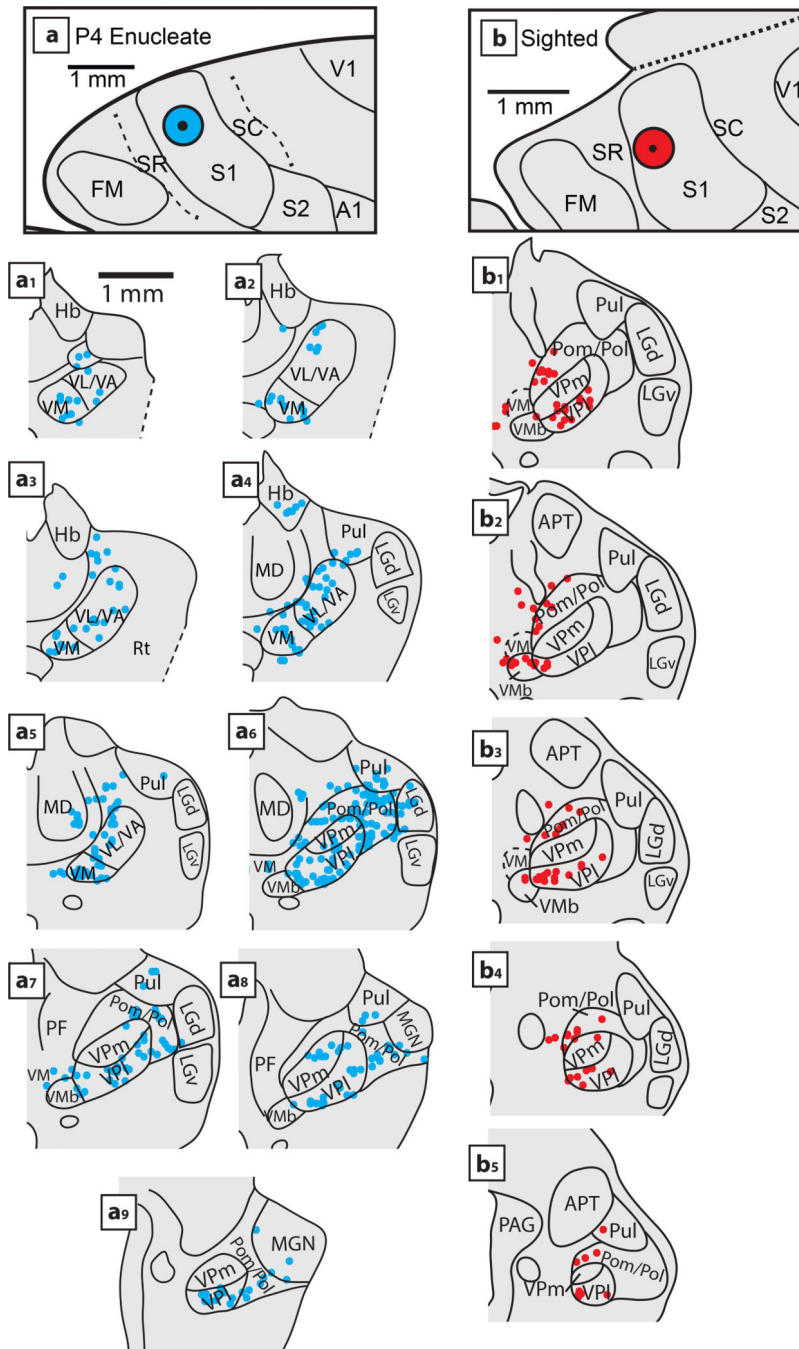
Figure 7:
Thalamocortical projections to S1 in P4 enucleates and sighted controls. (a) Fluoro-ruby injection in S1 of P4 enucleated *Monodelphis domestica*. (a$_1$-a$_9$) Rostral to caudal progression of thalamic sections containing retrogradely labeled neurons projecting to S1. Note that label in VP is mostly in the lateral division of the nucleus indicating that the medial injection site in S1 was in the representation of the body and limbs. Compared to sighted animals, enucleates show much stronger projections from VL/VA (a$_1$-a$_5$) and the neurons lateral to VP in Pom/Pol (a$_6$-a$_9$). (b) Location of retrogradely labeled neurons in the

thalamus projecting to S1 in a sighted opossum, adapted from Dooley et al., 2014. Thalamic neurons projecting to S1 primarily originate from VP and the medial portion of Pom/Pol. Note the reduced rostral/caudal extent of projections in bilateral enucleates compared to sighted animals. In sighted animals, sparse or no projections from VL/VA to S1 are observed.
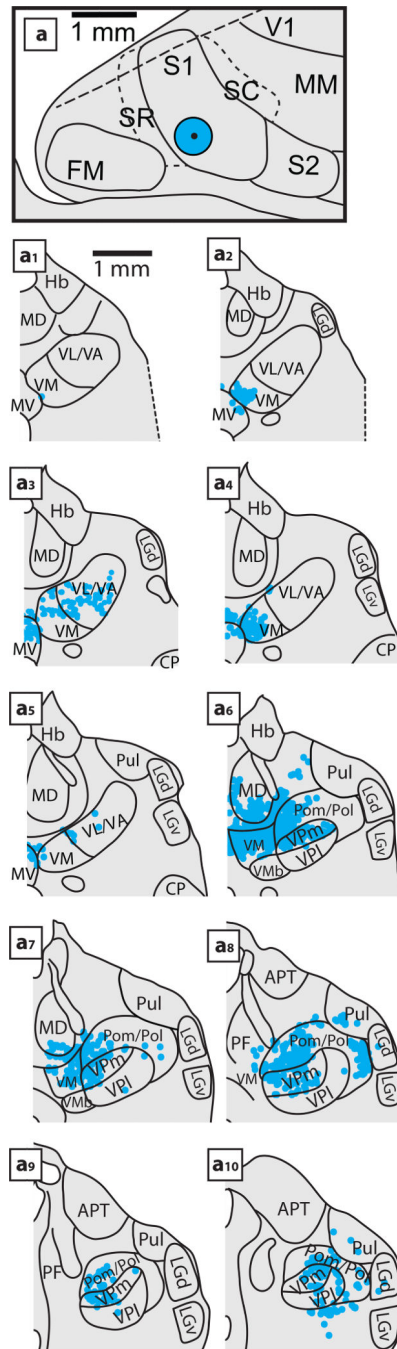
Figure 8:
Location of retrogradely labeled neurons in the thalamus resulting from an injection of CTB in S1. (a) CTB injection of P4 enucleated *Monodelphis domestica*. (a_1-a_{10}) Rostral to caudal progression of thalamic sections containing retrogradely labeled neurons projecting to S1. Most labeled neurons in VP are in the medial division indicating that the injection in S1 was in the face representation. Similar to Figure 7, there is an increase in neurons from VL/VA, medial thalamic nuclei, and neurons lateral to VP projecting to S1. A photograph of neurons in a_8 is shown in Figure 3. Conventions as in Figure 7.
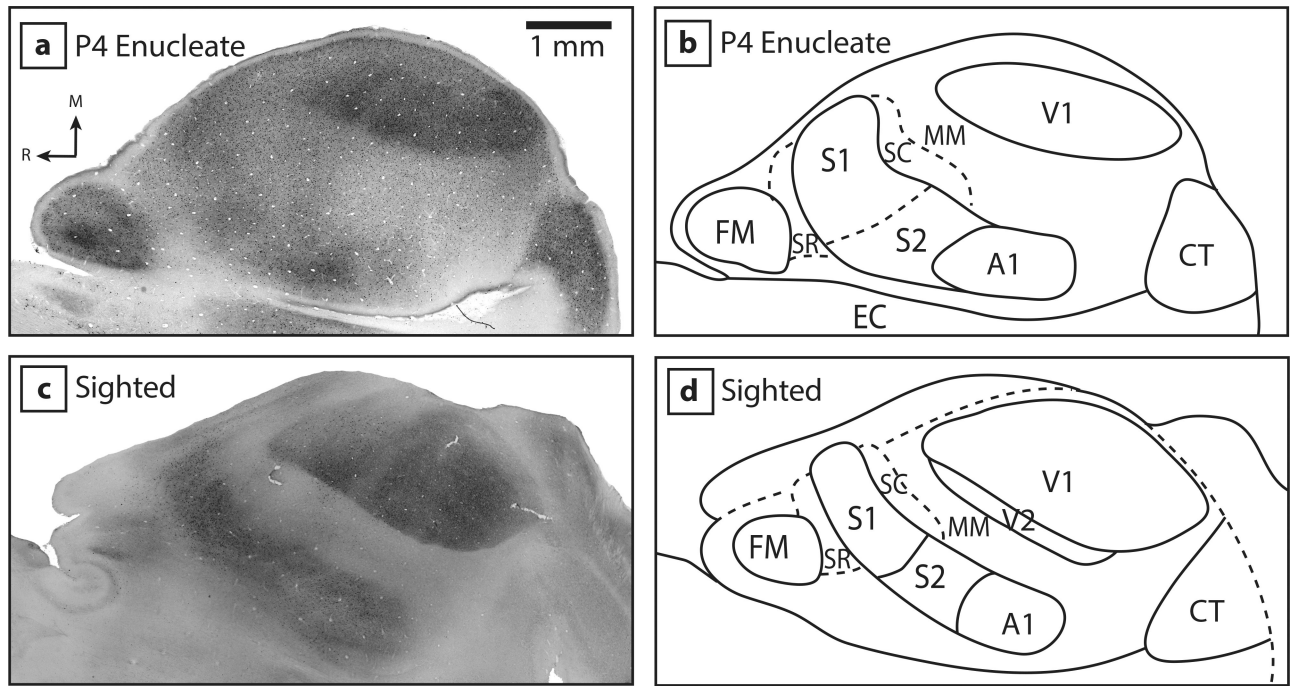
Figure 9:
Cortical field boundaries in a P4 enucleate (a and b) and sighted (c and d) *Monodelphis domestica* as revealed with parvalbumen (PV) stained tissue. This stain is particularly good for revealing the boundaries of V1 and S1. The reconstructions in b and d are taken from the entire series of stained sections since a single section cannot always reveal all of the boundaries. As described previously (Karlen & Krubitzer, 2009), V1 in enucleates is smaller and somatosensory cortex is enlarged compared to sighted animals. Rostral is to the left and medial is to the top. See Table of abbreviations.
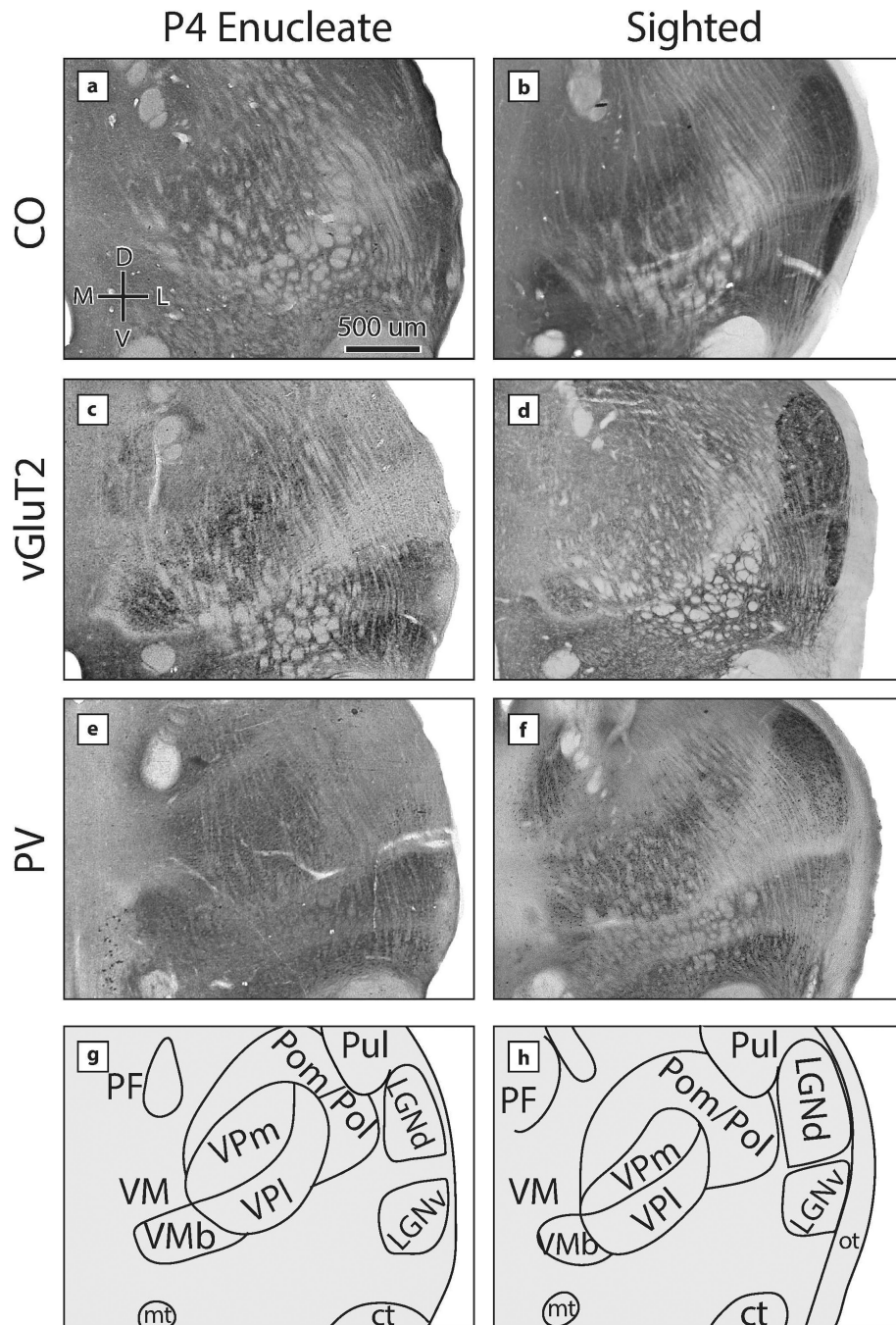
Figure 10:
Histological staining for CO (a and b), vGluT2 (c and d) and PV (e and f) in the thalamus in P4 enucleates (left) and sighted animals (right). For each group, a representative thalamic section is shown through the core of VP and LGd with an illustration labeling the different nuclei below (g, h). Notably, both LGd and LGv are not visible in vGluT2 and PV stained tissue in enucleates (c, e) and faintly visible in CO stained tissue (a), while they are clearly visible with all stains in sighted animals (b, d, f). Further, the optic tract is not present in the thalamus in enucleates. Dorsal is up, medial to the left.
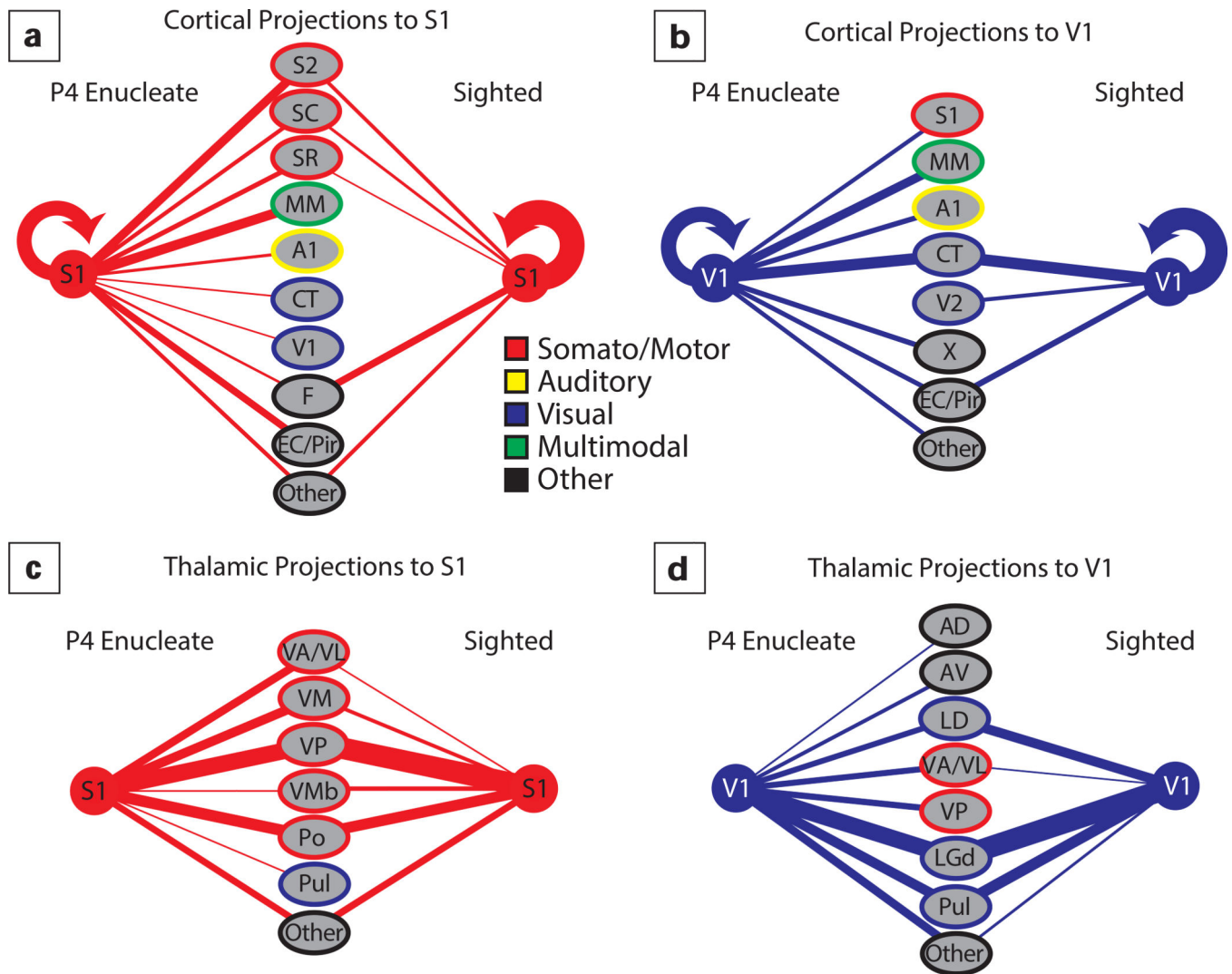
Figure 11:
Summary of all cortical (a, b) and thalamic (c, d) projections to S1 and V1 in both enucleates and sighted animals. Connections to S1 and V1 are shown if they represent more than 1% of the total number of labeled cells. Line thickness corresponds to connection strength. Colored outlines of cortical areas and thalamic nuclei indicate the modality generally associated with that area in a normal animal. Connectional data to V1 adapted from Karlen, Kahn and Krubitzer, 2006.

Table 1:

Tracer Injections

Details of the location, volume, and five tracer injections into S1 of P4 enucleates. Similar tracer injections, were made into S1 of sighted opossums as part of a previous studies (for details, see Table 2 of Dooley et al., 2013 and Dooley et al., 2014).

	Tracer	Injection Location	Tracer Volume	Number of Labeled Sections in:	
				Cortex	Thalamus
Case 1	FE	S1 medial	0.30	6	10
Case 2	CTB	S1 lateral	0.15	8	10
Case 3	CTB	S1 lateral	0.15	6	10
Case 4	CTB	S1 medial	0.15	6	8
Case 5	FR	S1 medial	0.30	0	9

TABLE 2

Antigen	Immunogen	Source, host species, catalog No., RRID	Dilution factor
Parvalbumin	Purified frog muscle parvalbumin	Sigma-Aldrich, mouse monoclonal antiparvalbumin, P3088, RRID: AB_477329	1:2000
Vesticular glutamate transporter 2	Recombinant protein from rat vGluT2	Millipore, mouse monoclonal antivGluT2, MAB5504, RRID: AB_2187552	1:5000

TABLE 3

	ENUCLEATES						SIGHTED		T-TEST
	Case 1	Case 2	Case 3	Case 4	Mean	SE	Mean	SE	
S1	47.8 *131*	23.6 *842*	18.0 *525*	33.7 *670*	**30.8**	*6.5*	**72.6**	*13.1*	***P = 0.01***
S2	13.9 *38*	11.7 *418*	14.5 *421*	15.3 *304*	**13.8**	*0.8*	**4.8**	*5.2*	***P = 0.02***
SC	5.5 *15*	5.3 *187*	2.9 *85*	7.7 *154*	**5.3**	*1.0*	**3.9**	*3.4*	*P = 0.98*
SR	8.0 *22*	6.2 *222*	6.8 *199*	4.9 *98*	**6.5**	*0.6*	**1.6**	*0.6*	*P = 0.18*
MM	15.3 *42*	16.2 *578*	24.4 *709*	9.8 *194*	**16.4**	*3.0*	**0.2**	*0*	***P < 0.01***
A1	4.0 *11*	2.0 *71*	2.7 *79*	7.3 *146*	**4.0**	*1.2*	**0.4**	*0.3*	***P = 0.02***
CT	0.0 *0*	2.5 *90*	6.0 *176*	1.9 *38*	**2.6**	*1.3*	**0**	*0*	***P = 0.05***
V1	0.7 *2*	2.8 *98*	1.0 *30*	0.5 *10*	**1.3**	*0.5*	**0**	*0.1*	*P = 0.09*
FM	1.8 *5*	5.5 *195*	5.6 *164*	1.0 *19*	**3.5**	*1.2*	**10.6**	*14*	*P = 0.31*
EC/Pir	1.5 *4*	19.6 *697*	8.0 *232*	12.4 *246*	**10.3**	*3.8*	**0.5**	*0.9*	***P = 0.03***
OTHER	1.5 *4*	4.6 *163*	10.0 *290*	5.5 *110*	**5.4**	*1.8*	**5.3**	*1.0*	*P = 0.66*

Percentage of labeled cells (upper) and number of counted cells (lower, italicized) from the above listed cortical areas projecting to S1 for all P4 enucleated animals, along with the percentages reported for sighted animals. For the T-Test column, bold indicates a significant difference.

TABLE 4

| | ENUCLEATES | | | | | | | SIGHTED | | T-TEST |
	Case 1	Case 2	Case 3	Case 4	Case 5	Mean	SE	Mean	SE	
VA/VL	11.1 *14*	6.7 *96*	28.3 *188*	1.9 *12*	14.5 *61*	**12.5**	*4.5*	**2.0**	*1.0*	**P = 0.03**
VM	4.0 *5*	27.3 *392*	15.2 *101*	14.3 *76*	15.6 *66*	**15.3**	*3.7*	**4.9**	*2.2*	**P = 0.03**
CL	1.6 *2*	7.0 *100*	1.7 *11*	0.0 *0*	3.1 *13*	**2.7**	*1.2*	**1.3**	*0.8*	P = 0.36
MD	0.8 *1*	6.7 *97*	1.1 *7*	0.0 *0*	1.9 *8*	**2.1**	*1.2*	**0.6**	*0.6*	P = 0.29
VP	48.4 *61*	21.1 *303*	18.7 *124*	70.0 *371*	26.8 *113*	**37**	*9.8*	**57.5**	*4.7*	P = 0.08
VMb	2.4 *3*	0.3 *4*	1.8 *12*	5.1 *27*	0.0 *0*	**1.9**	*0.9*	**6.0**	*1.9*	P = 0.10
Pom/Pol	25.4 *32*	21.8 *314*	28.2 *187*	7.0 *37*	21.1 *89*	**20.7**	*3.7*	**19.2**	*2.9*	P = 0.74
LGd	0.8 *1*	0.2 *3*	0.5 *3*	0.0 *0*	3.1 *13*	**0.9**	*0.6*	**0.0**	*0.0*	P = 0.11
Pul	1.6 *2*	1.0 *15*	0.0 *0*	0.0 *0*	8.1 *34*	**2.1**	*1.5*	**0.2**	*0.2*	P = 0.18
Other	4.0 *5*	7.9 *114*	4.7 *31*	1.7 *9*	5.9 *25*	**4.8**	*1.0*	**8.3**	*1.6*	P = 0.24

Percentage of labeled cells (upper) and number of counted cells (lower, italicized) from the above listed thalamic nuclei projecting to S1 for all P4 enucleated animals, along with the percentages reported for sighted animals. For the T-Test column, bold indicates a significant difference.